ELSEVIER

Advances in Colloid and Interface Science
96 (2002) 101–129

ADVANCES IN COLLOID AND INTERFACE SCIENCE

www.elsevier.com/locate/cis

Stability of draining plane-parallel films containing surfactants

Dimitrina S. Valkovska, Krassimir D. Danov*, Ivan B. Ivanov

Laboratory of Chemical Physics & Engineering, Faculty of Chemistry, University of Sofia, 1164 Sofia, Bulgaria

Abstract

The stability of partially mobile draining thin liquid films with respect to axisymmetric fluctuations was studied. The material properties of the interfaces (Gibbs elasticity, surface and bulk diffusions) were taken into account. When studying the long wave stability of films, the coupling between the drainage and perturbation flows was considered and the lubrication approximation was applied. Two types of wave modes were examined: radially-bounded and unbounded waves. The difference between the thickness of loss of stability, h_{st}, the transitional thickness, h_{tr}, at which the critical wave causing rupture becomes unstable, and the critical thickness, h_{cr}, when the film ruptures, is demonstrated. Both the linear and the non-linear theories give $h_{st} > h_{tr} > h_{cr}$. The numerical results show that the interfacial mobility does not significantly influence the thickness of the draining film rupture. The interfacial tension and the disjoining pressure are the major factors controlling the critical thickness. The available experimental data for critical thicknesses of foam and emulsion films show excellent agreement with the theoretical predictions. The important role of the electromagnetic retardation term in the van der Waals interaction is demonstrated. Other published theories of the film stability are discussed.

Keywords: Draining thin films; Stability; Critical thickness; Influence of surfactants; Interfacial mobility; Surface elasticity and diffusion

* Corresponding author. Tel.: +359-2-9625310; fax: +359-2-9625643.
E-mail address: kd@ltph.bol.bg (K.D. Danov).

0001-8686/02/$ - see front matter
PII: S0001-8686(01)00077-X

Contents

1. Introduction 102
2. Mathematical model: lubrication approximation 106
3. Linear stability analysis of draining plane-parallel films 108
   3.1. Bounded waves: stability thickness 110
   3.2. Unbounded waves: stability, transitional and critical thickness 114
4. Numerical results and discussion 119
5. Conclusions 127
Acknowledgements 127
References 128

1. Introduction

Studies on the stability of thin liquid films are of great importance for understanding the stability of colloidal systems such as foams and emulsions [1,2]. A great number of experimental and theoretical investigations are performed in order to elucidate the influence of the different factors (surfactant properties and concentration, film radius, bulk and surface diffusion, surface viscosity, etc.) on the critical thickness of the film rupture (for detailed review see Maldarelli and Jain [3], Kralchevsky et al. [4], Danov et al. [5]). Nevertheless, there are still some 'open questions' which have not been explained.

Two processes determine the lifetime of liquid films: thinning and breaking. The thinning of films is a result of drainage of the liquid under the action of the some external forces. When the film goes down to a thickness of the order of 100 nm, the intermolecular forces, such as van der Waals attraction, electric double-layer repulsion, etc., also come into operation [6–8]. The van der Waals attraction increases the drainage rate while the electrostatic repulsion decreases it. On further thinning, some films reach the primary equilibrium thickness (when border suction, i.e. capillary pressure, equals the disjoining pressure, Π) or collapse between 10 and 50 nm [4,5]. The film instability is attributed to mechanical perturbations or thermal fluctuations, which lead to corrugation of the film surfaces. Generally speaking, the elasticity and the viscosity of the film interfaces and the viscosity of the bulk phases damp the amplitudes of the perturbations. On the contrary, if the disjoining pressure, Π, decreases for the smaller local film thickness the corrugations of the interfaces will grow faster. The interplay of both contributions determines the stability of thin liquid films.

In early studies, the instability was analysed by examining the variation of the free energy with respect to the film thickness [9]. Such results have thermodynamic origin and are therefore valid for non-draining thin films. Frenkel [9] showed that the necessary thermodynamic condition for instability is $\Pi' \equiv \partial \Pi / \partial h > 0$, where h is the unperturbed film thickness of a planar film. This result is valid for

unbounded plane-parallel non-draining films. Let us assume that the real corrugated profile can be expanded in Fourier series, i.e. can be represented as superposition of periodic waves as the one shown in Fig. 1. At a given position r, there will be at least two forces acting on the surfaces: (i) the local capillary pressure, tending to flatten the surface, i.e. to stabilize the wave, and (ii) the local disjoining pressure will tend to deepen and destabilize the corrugation, if it is negative (i.e. van der Waals attraction). Since both effects depend on the film thickness, for a given thickness, h, and thereby — given value of Π', there will be both stable and unstable waves depending on which effect prevails. It is possible that one of the waves becomes unstable exactly at this thickness. Let its wave number be $k_{st}(h)$ (the subscript 'st' stands for 'stability' and it is used hereafter to denote the values of the variables corresponding to transition between stable and unstable regimes). For k_{st} Frenkel obtained

$$k_{st} \equiv (2\Pi'/\sigma)^{1/2} \tag{1}$$

where σ is the interfacial tension [9]. Every unstable wave can in principle break the film, when the two surfaces 'touch' each other, provided that there is no repulsive interaction strong enough to prevent the film rupture. For this to happen the amplitude of the film must increase from the value it had at the moment, when it became unstable, until it becomes equal to $h/2$ (for symmetric waves, the so-called 'squeezing mode', shown in Fig. 1). This process takes time, which is called the film breaking time, t_{br} [10]. The calculation of t_{br} is already a hydrodynamic problem. For the case of tangentially immobile interfaces and small perturbations (i.e. when the linear stability analysis can be used) the breaking time was calculated by Vrij [11]. (The role of the surface mobility, when the film is stabilized by soluble and insoluble surfactants is discussed in Maldarelli and Jain [3], Ivanov et al. [12], Lu and Cates [13].) Vrij [11] noted that for a given film thickness, h, the corrugations with a wave number $k_{mrg} = k_{st}/\sqrt{2}$ will grow faster than all others, and this mode, called 'the most rapidly growing thickness fluctuation', determines t_{br}. However, a linear analysis ceases to be valid at finite shape deformation, i.e. when the corrugation amplitudes become comparable with the film thickness. Williams and Davis [14] and Wit et al. [15] showed that the solution of the non-linear evolution equations, derived asymptotically from the Navier–Stokes equations, gives a smaller film breaking time for non-draining films than that predicted from the linear theory.

If the non-draining film is bounded, the wavelength must be smaller than the film radius, R, so that the stability wave number, k_{st}, cannot be smaller than α/R, where the numerical coefficient α depends on the geometry of the fluctuation mode. (For radially bounded axisymmetric film α is equal to the first zero of the zeroth-order Bessel function, $\alpha_1 \approx 2.4048$ and $k_{st} = \alpha_1/R$.) This limitation implies that, unlike in the case of unbounded films, unstable waves on bounded films will not be present at all thicknesses. The maximum thickness, h_{st}, at which the first

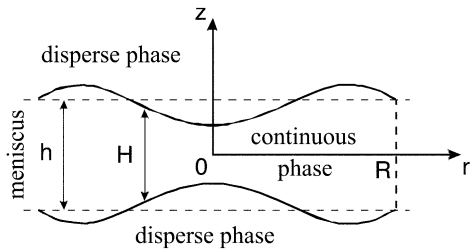

Fig. 1. Sketch of drainage film of radius, R, and unperturbed thickness, h. The fluctuations of local film thickness, H, are enlarged.

unstable wave will appear, can be calculated from Frenkel's equation [Eq. (1)]. For axisymmetric waves it is [16]

$$h_{st} = \left(\frac{A_H R^2}{\pi \alpha_1^2 \sigma}\right)^{1/4} \approx 0.4844\left(\frac{A_H R^2}{\sigma}\right)^{1/4} \tag{2}$$

where the van der Waals disjoining pressure is presented through the Hamaker constant, A_H, by the form:

$$\Pi = -A_H/(6\pi h^3) \tag{3}$$

Therefore, if the film thickness, h, is smaller than h_{st} the film is unstable and in the opposite case — it is stable.[1]

Surfactants damp the interfacial mobility and for non-draining films they lead to smaller velocity of corrugation growth. Therefore, the surfactants play important roles on the film breaking time, t_{br}, and stabilize the non-draining films. In the case of draining films the role of surfactants on the thickness of film rupture is less pronounced (see Section 4).

The stability problem for films, formed between colliding bubbles in foams or drops in emulsions, is complicated by the fact that these films are usually thinning (under the action of the external force and the disjoining pressure) before coalescence occurs. Vrij [11] and Vrij and Overbeek [17] realized that even when a given wave becomes unstable, a finite time is needed for the corrugations on the two film surfaces to develop and 'touch' each other so that the film breaks. During this time the average thickness h of the thinning film decreases so that the rupture occurs at

[1] By using an approximate model, in 1962, Scheludko [16] derived an equation for what he considered as critical thickness of rupture of a draining film, h_{cr}. In the present notations his result can be written as $h_{cr}^4 = A_H\lambda^2/(128\pi\sigma)$ where λ is the length of the surface wave, causing the rupture. Replacing λ by the respective wave number k, $\lambda = 2\pi/k$, and introducing Π' by means of Eq. (3), it is easy to show that Scheludko's equation is equivalent to $k^2 = \pi^2\Pi'/(16\sigma)$, which is the same as Frenkel's equation [Eq. (1)] , exception made for the numerical coefficient, hence, Scheludko actually re-derived (approximately) Frenkel's condition for appearance of any unstable wave in a non-draining film, rather than the critical thickness of rupture, h_{cr} of a draining film (for more details on h_{cr} see Section 3.2).

a critical thickness, h_{cr}, which is smaller than the stability thickness. Hence, the hydrodynamic problems for film drainage and corrugation growth must be solved simultaneously. Vrij [11] and Vrij and Overbeek [17] obtained a solution by using an ingenious, though semi-empirical procedure. They used Reynolds equation [see Eq. (13) below] to calculate the drainage time, t_{dr}, i.e. the time needed by a planar film with tangentially immobile surfaces to thin down from an unspecified initial thickness to a given thickness h and their equation for the breaking time of a non-draining film, t_{br}, at that thickness (see above). While the former decreases with increasing h, the latter obviously increases, so that their sum goes through a minimum as a function of h. The authors further assumed: (i) that this minimum value is the life time, t_m, of the draining film and (ii) that it is equal to the draining time until film rupture, i.e. they calculated the critical thickness, h_{cr}, as the thickness, which the draining planar film will reach for time t_m. In this way they managed to derive the following simple expression for the critical thickness in the case of van der Waals disjoining pressure

$$h_{cr} \approx 0.2069\left(\frac{A_H^2 R^2}{\sigma P_c}\right)^{1/7} \tag{4}$$

valid when the capillary pressure, P_c, is much larger that the disjoining pressure calculated at h_{cr}.

A short time later Ivanov et al. [12] published a generalization of the Vrij [11] and Vrij and Overbeek [17] approach. The authors [12] used the results from the linear stability analysis of non-draining films and formulated a systematic theoretical procedure for calculation of the critical thickness. This allowed them also to account for the effect of surface mobility (i.e. of the dissolved surfactant) on the film drainage and wave motion. A detailed explanation of this procedure is given in Section 3.2. The main problem that remained unsolved in this paper is that the coupling between drainage and wave motion was not fully accounted for, although the authors used a quasi-steady procedure, which permitted establishing connection between the two motions [see e.g. Eq. (31) below]. However, since they used the dispersion relationship of non-draining films to examine the stability of thinning films, they actually neglected the contribution of the dynamic pressure in the draining film on the wave motion. Following Ivanov et al. [12] in this study we will distinguish the following three thicknesses: the stability thickness, h_{st} (the boundary between the regions of stability and instability); the critical thickness, h_{cr} (the thickness of the film at the moment of its rupture); the transitional thickness, h_{tr} (the thickness at which the critical wave becomes unstable, for details see Section 3.2).

The coupling effect was accounted for by Gumerman and Homsy [18] and Malhotra and Wasan [19] by using linear analysis for the calculation of the stability thickness, h_{st}, i.e. they studied only the transition from stability to instability, but not the film rupture per se. Their studies were done for bounded axisymmetric

draining film with tangentially immobile interfaces, i.e. the role of the surface mobility was disregarded. The wave spectrum they obtained is of course discrete (the perturbations are bounded at the film periphery), whereas for unbounded films it is continuous.

In the present study we have tried to formulate a more general and systematic approach by removing some of the limitations of the previous theories, such as the neglect of the hydrodynamic coupling or the assumption for tangential surface immobility. We have also analysed the applicability of some approximations, including also the validity of the linear stability approximation. In Section 2 the main equations needed to describe the shape, the evolution and the stability of draining liquid films in the presence of surfactants are formulated in lubrication approximation. In the beginning of Section 3 they are linearized with respect to the perturbations, i.e. linear stability analysis is applied. In Section 3.1 the onset of instability of radially-bounded axisymmetric films is studied and the respective stability thickness is calculated. The same is done for unbounded films in Section 3.2, but in addition the critical thickness of rupture is calculated as a function of the system parameters. The results of the calculations, based on the proposed theories, are compared with the available experimental data for foam and emulsion films in Section 4. No adjustable parameters are used and the agreement between theory and experiment is excellent. Probably the only essential shortcoming of the theory proposed here is the use of the linear stability approach. It can be avoided by using the non-linear stability analysis. This issue is briefly discussed in Section 4 and it is shown that at least for unbounded films with only attractive (van der Waals) disjoining pressure the linear theory leads to very satisfactory results.

2. Mathematical model: lubrication approximation

The mathematical model for the description of the drainage and stability of a symmetric thin liquid film is based on the following assumptions. The processes of film thinning and fluctuations growth are so slow that the Reynolds number is small enough to allow neglecting the convective terms in the equation of fluid motion. The local film thickness, H, is much smaller than the typical film radius, R. Due to the lower viscous dissipation the amplitudes of the longer waves increase faster then those of the shorter waves. For that reason the long wave approximation is used for calculation of the perturbation flow. In addition axial symmetry of drainage and perturbation flows is considered. Therefore, the common lubrication approximation can be used [20–25]. In this approximation the pressure, P, in the film phase depends only on the radial co-ordinate, r, and time, t: $P = P(r,t)$, where Orz is a cylindrical co-ordinate system with vertical co-ordinate z (Fig. 1). After integration of the equations of fluid motion and continuity, with account for the corresponding kinematic boundary conditions, the integrated bulk continuity equation takes the form [20–25]

$$\frac{\partial H}{\partial t} + \frac{1}{r}\frac{\partial}{\partial r}\left[rH\left(U - \frac{H^2}{12\eta}\frac{\partial P}{\partial r}\right)\right] = 0 \tag{5}$$

where η is the dynamic viscosity and U is the radial component of the surface velocity.

The film is stabilized by surfactant dissolved only in the continuous phase. The surfactant distribution is calculated by solving the bulk diffusion equation along with the surfactant mass balance at the film surfaces. The assumption that the Peclet number for the draining and fluctuation processes is small is equivalent to small deviations of the surfactant concentration and the adsorption from their equilibrium values. In addition, the mechanism of adsorption has to be specified. In general, the surfactant adsorption involves two stages — diffusion of surfactant molecules from the bulk solution to the subsurface and transfer of the surfactant molecules from the subsurface to the surface. It is proven in the literature [5,20] that the time limiting process for the adsorption processes in thin liquid films stabilized by non-ionic and ionic surfactants is the diffusion. The reason is the overlapping of the diffuse layers on the two interfaces, which results in a smaller concentration gradient and thereby — slower diffusion [5,20]. For the same reason the subsurface surfactant concentration coincides with the bulk concentration in the film — the latter greatly facilitates the derivations, since for low molecular weight surfactants the adsorption, Γ, can be connected to the surfactant concentration in the film, c, through the adsorption isotherm. Using these assumptions and the solution of the diffusion problem, the dependence of the adsorption gradient on the surface velocity, U, and the local film thickness, H, is obtained [12,20,21,23].

The boundary condition for the balance of the surface excess linear momentum takes into account the influence of the surface viscosity (Boussinesq effect) and the surface tension gradient (Marangoni effect). The role of the surface viscosity is estimated by the dimensionless parameter $\eta_s h/(\eta\lambda^2)$, where the sum of the interfacial shear, η_{sh}, and dilatational, η_{dil}, viscosity, is the total surface viscosity, $\eta_s \equiv \eta_{sh} + \eta_{dil}$, and λ is the wavelength. For thin films and long waves this parameter is small and the role of the interfacial viscosity can be neglected. Then for small deviations from equilibrium the tangential stress balance boundary condition simplifies to [23–25]

$$\frac{H}{12\eta}\frac{\partial P}{\partial r} = -\frac{U}{h_s + bH} \tag{6}$$

The parameters b, h_s, h_a and E_G account for the effect of the surfactants on the film drainage and stability and they are defined trough the relationships:

$$b \equiv \frac{3\eta D}{h_a E_G}, \quad h_s \equiv \frac{6\eta D_{cs}}{E_G}, \quad E_G \equiv -\frac{\partial\sigma}{\partial \ln\Gamma}, \quad h_a \equiv \frac{\partial\Gamma}{\partial c} \tag{7}$$

Neither of the parameters in the definitions [Eq. (7)] depends on the film thickness — they all are determined by the physicochemical properties only of the

surfactant solution. The effect of the bulk diffusion is accounted for by the parameter b, where D is the bulk diffusion coefficient. The slope of the adsorption isotherm is h_a and E_G is the Gibbs elasticity. The influence of the surface diffusion is given by the parameter h_s, defined through the collective surface diffusion coefficient, D_{cs}, which is proportional to the gradient of the surface chemical potential, μ_s, and therefore it depends on the adsorption. The collective surface diffusion coefficient, D_{cs}, can be calculated from the relationship [26]

$$D_{cs} \equiv \frac{D_s}{k_B T} \frac{\partial \mu_s}{\partial \ln \Gamma} \tag{8}$$

where T is the temperature, k_B is the Boltzmann constant, and D_s is the surface self-diffusion coefficient. The last relationship has an important physical implication because σ can be eliminated from the expression [Eq. (7)] for E_G by using Gibbs adsorption isotherm: $d\sigma = -\Gamma d\mu_s$. Substituting this in the expression for h_s and using also Eq. (8), we obtain $h_s = 6\eta D_s/(k_B T \Gamma)$, i.e. the surface mobility is controlled (through h_s) directly by the surfactant adsorption, Γ, rather than by the Gibbs elasticity.

The normal stress boundary condition in the lubrication approximation reduces to the balance of the capillary pressure, P_c (of the drop or bubble surface outside of the film region), the pressure in the meniscus, P_m, the disjoining pressure, Π, the local capillary pressure, and the dynamic pressure, P, [21]:

$$P_m + P_c = P + \Pi + \frac{\sigma}{2r} \frac{\partial}{\partial r} \left(r \frac{\partial H}{\partial r} \right) \tag{9}$$

Gumerman and Homsy [18] and Malhotra and Wasan [19] took into account the viscous pressure term in the normal stress boundary condition [Eq. (9)]. The ratio between the capillary pressure and the viscous terms is measured by R/h, which is much higher than unity and the latter can be neglected.

It is important to note that in the lubrication approximation when the surfactants are soluble only in the continuous phase the viscous friction from the fluid in the drops is negligible compared to the friction from the continuous phase — hence, the emulsion system behaves as a foam [12,20,27–30]. This simplification is not valid when the viscosity of the disperse phase is much larger than the viscosity of the continuous phase — in the case of highly viscous oil emulsions [31].

Finally, the force balance closes the system of relations in Eqs. (5)–(9). For small Reynolds number it represents the balance of the hydrodynamic drag force and the external force, which acts on the film interfaces in process of thinning [20–23].

3. Linear stability analysis of draining plane-parallel films

The mathematical model in Section 2 entirely describes the draining flow parameters and the stability of the film with respect to long waves. We will present

the flow and shape quantities as superposition of the effects due to the drainage of the unperturbed planar film (basic flow) and the perturbations (corrugations). The contributions of the former effect will be denoted by subscript 'up' and those due to the later effect — by a subscript 'p': thus, for the pressure, velocity and local film thickness we will have P_{up}, U_{up} and H_{up}, and respectively, P_p, U_p and H_p. Then

$$P = P_{up} + P_p, \quad U = U_{up} + U_p, \quad H = H_{up} + H_p \tag{10}$$

In the linear stability approximation the governing equations for perturbations are linearized by assuming that the fluctuations are small. The coefficients of the resulting homogeneous system of equations are functions of the radial co-ordinate and time. Most experiments show that after the formation of a small almost plane-parallel film it thins without significantly changing its radius, R, and remaining essentially planar [4,12,20,32–34]. Hence, the stability problem can be simplified by considering a plane-parallel profile of the film in the unperturbed state. The basic parameters of the draining plane-parallel film have been obtained and the following relationships have been derived [12,20–23]:

$$\frac{\partial P_{up}}{\partial r} = -\frac{6\eta V r}{h^2[(1+b)h + h_s]} \tag{11}$$

$$U_{up} = \frac{(bh + h_s)Vr}{2h[(1+b)h + h_s]}, \quad H_{up} = h \tag{12}$$

The velocity of film thinning, $V = -\mathrm{d}h/\mathrm{d}t$, in Eqs. (9) and (10) is [12,20–23]

$$V = V_{Re}\left(1 + b + \frac{h_s}{h}\right), \quad V_{Re} \equiv \frac{2h^3}{3\eta R^2}[P_c - \Pi(h)] \tag{13}$$

where V_{Re} is the velocity of approach of a plane-parallel film with tangentially immobile interfaces thinning under the combined action of the capillary and the disjoining pressure.

To obtain the equations of the linear stability problem Eq. (10) and the relationships for the parameters in the unperturbed state [Eqs. (11)–(13)] are substituted into the integrated bulk continuity equation [Eq. (5)] and the tangential and normal stress boundary conditions, Eqs. (6) and (9). The resulting problem is linearized with respect to the small perturbations. The final form of the linear stability equations reads

$$\frac{\partial H_p}{\partial t} + \frac{V}{2h}\frac{(3+b)h + h_s}{(1+b)h + h_s}\frac{1}{r}\frac{\partial}{\partial r}\left(r^2 H_p\right) + \frac{h}{r}\frac{\partial}{\partial r}\left[r\left(U_p - \frac{h^2}{12\eta}\frac{\partial P_p}{\partial r}\right)\right] = 0 \tag{14}$$

$$U_p = -\frac{h(bh + h_s)}{12\eta}\frac{\partial P_p}{\partial r} + \frac{V}{2h}\frac{2bh + h_s}{(1 + b)h + h_s} r H_p \tag{15}$$

$$P_p + \Pi' H_p + \frac{\sigma}{2r}\frac{\partial}{\partial r}\left(r\frac{\partial H_p}{\partial r}\right) = 0 \tag{16}$$

where the derivative of the disjoining pressure is defined as: $\Pi' \equiv d\pi/dh$.

If the expression for the perturbation of the surface velocity [Eq. (15)] is substituted into the integrated mass balance equation [Eq. (14)] the latter reduces to:

$$\frac{\partial H_p}{\partial t} + \frac{V}{2h}\frac{3(1 + b)h + 2h_s}{(1 + b)h + h_s}\frac{1}{r}\frac{\partial}{\partial r}\left(r^2 H_p\right) = \frac{h^2[(1 + b)h + h_s]}{12\eta}\frac{1}{r}\frac{\partial}{\partial r}\left(r\frac{\partial P_p}{\partial r}\right) \tag{17}$$

The second term in the left-hand side of Eq. (17) takes into account the coupling between the basic and perturbation flows. It will be called here and hereafter 'dynamic pressure term'. The formal substitution, $V = 0$, in Eq. (17) leads to the equation for the fluctuation of the thickness in a non-draining film.

A major problem when obtaining the solution for the shape of the perturbations is to choose the boundary condition they must satisfy at the film rim (at $r = R$). There are, at least, two possibilities and both have some physical ground. One of them is to assume that the amplitude at $r = R$ is zero, i.e. that the waves are bounded. The physical reason for this can be the following. The amplitude is enhanced by the van der Waals disjoining pressure, which according to Eq. (3) strongly decreases as the thickness increases. If there is a sharp transition between the film and the meniscus, in the meniscus region, at $r > R$, the local thickness will increase quickly with r and will be much larger than the film thickness h. Therefore, the disjoining pressure there must be zero and the amplitude of the wave must be the same as at a single interface, which is $0.1 \div 0.5$ nm (see Section 3.2). Compared to the amplitude inside the film, which is of the order of h, this value is essentially zero. It is possible, however, to consider the fluctuations also as unbounded waves. Indeed, in reality there is no sharp boundary between the film and the meniscus (see Ivanov and Dimitrov [20], Ivanov et al. [21]). If so, the amplitude must decay gradually with r when going from the film to the meniscus region. We have used both models in Section 3. Fortunately, it turned out that the critical wavelength is much smaller than the film radius (see Section 4), so that the boundary condition at the film rim has little significance.

3.1. Bounded waves: stability thickness

According to the stability analysis if $\partial H_p/\partial t > 0$ the amplitude of the fluctuation in the film thickness will grow and if $\partial H_p/\partial t < 0$ the amplitude will decrease. The

stability limit, h_{st}, is reached when $\partial H_p/\partial t = 0$. When $\partial H_p/\partial t = 0$ the system of relations, Eqs. (16) and (17), has the following first integral

$$\frac{V}{2h}\frac{3(1+b)h+2h_s}{(1+b)h+h_s}rH_p + \frac{h^3[(1+b)h+h_s]}{12\eta}\frac{\partial}{\partial r}\left[\Pi' H_p + \frac{\sigma}{2r}\frac{\partial}{\partial r}\left(r\frac{\partial H_p}{\partial r}\right)\right] = 0 \tag{18}$$

which generalizes the respective problem in Gumerman and Homsy [18], Malhotra and Wasan [19] by taking into account the influence of surfactants.

In the case of radially-bounded waves $H_p = 0$ at the film ring (at $r = R$) one can represent the perturbations as a superposition of Fourier–Bessel modes [18,19]:

$$H_p = \sum_{k=1}^{\infty} H_k J_0\left(\alpha_k \frac{r}{R}\right) \tag{19}$$

where J_n is the n-order Bessel function and α_k are the roots of the zeroth-order Bessel function, $J_0(\alpha_k) = 0$. The substitution of the series [Eq. (19)] into Eq. (18) leads to the following homogeneous system of equations for the unknown constants, H_k:

$$\frac{1}{2}\left[\frac{(3+b)h+h_s}{(1+b)h+h_s} + \frac{2bh+h_s}{(1+b)h+h_s}\right]\sum_{k=1}^{\infty} a_{k,n}H_k - H_n + \frac{h^3\alpha_n^2}{24\eta VR^4}[(1+b)h+h_s](\sigma\alpha_n^2 - 2R^2\Pi')H_n = 0, \quad n = 1,2,\ldots \tag{20}$$

where the coefficients $a_{k,n}$ are defined as [18,19]

$$a_{n,n} = 1, \quad a_{k,n} = \frac{2\alpha_k\alpha_n}{\alpha_k^2 - \alpha_n^2}\frac{J_1(\alpha_k)}{J_1(\alpha_n)}, \quad k \neq n \tag{21}$$

The formal limit, $b = 0$ and $h_s = 0$, reduces the problem [Eqs. (20) and (21)] to the respective equations for tangentially immobile interfaces [18,19].

The discrete spectrum of Eq. (18) is found from the dispersion relationship obtained by setting the determinant of the matrix of the infinite system equal to zero. The stability thickness, h_{st}, is the largest value of this spectrum because for all thicknesses smaller than h_{st} the film is unstable. From mathematical viewpoint the solution of the stability problem is correctly determined. However, we will not use this method of calculation because of the following two problems. The first problem that appears is a numerical one. When calculating the stability thickness numerically, only final number, N, of equations from the system [Eqs. (20) and (21)] can be used. Since the numerical procedure converges very slowly, the calculated value of h_{st} depends strongly on N. The second problem arises from the form of the solution [Eq. (19)], which is not general. As shown below, Eq. (18) has two independent characteristic functions and, therefore, it requires two boundary

conditions at the film periphery. One of the boundary conditions is that the fluctuation of the film thickness at the film rim is zero. The second one can be different. For example, if the fluctuations stick smoothly to the meniscus at the film rim, then $\partial H_p/\partial r = 0$ at $r = R$. Another boundary condition can be the assumption that the perturbation in the dynamic pressure vanishes at the film boundary, i.e. $P_p = 0$ at $r = R$, which was used in [18,19] [it is derived by substitution of the series Eq. (19) into Eq. (16)]. In order to avoid these problems the exact general solution of Eq. (18) is found below.

Our approach is based on the exact general solution of Eq. (18). The third order differential equation [Eq. (18)] has a general solution, which is a superposition of three independent characteristic functions, F_1, F_2 and F_3. One of them (we assume it is F_3) is singular at $r = 0$. Therefore, $H_p = A_1F_1 + A_2F_2$, where the constants A_1 and A_2 are determined by the boundary conditions at the film periphery. According to the Frobenius method [35] the characteristic functions are presented as series of even powers of the radial co-ordinate, r:

$$F_i = \sum_{k=0}^{\infty} C_{i,k} r^{2k}, \quad i = 1,2 \tag{22}$$

where $C_{i,k}$ are constants. After substituting the series [Eq. (22)] into Eq. (18) and equalizing the coefficients before the equal powers of r, the following exact recurrent relationships for $C_{i,k}$ are derived

$$C_{i,k+2} = -\frac{1}{8(k+2)^2} \times \left\{ \frac{4R^2\Pi'}{\sigma} C_{i,k+1} + \frac{24\eta V R^4}{\sigma h^3 (k+1)} \frac{3(1+b)h + 2h_s}{[(1+b)h + h_s]^2} C_{i,k} \right\} \tag{23}$$

where $i = 1, 2$ and $k \geq 0$. The characteristic functions are specified within a constant. Hence, in order to choose two independent characteristic functions the initial coefficients can be taken to be: $C_{1,0} = 0$, $C_{1,1} = 1$, $C_{2,0} = 1$ and $C_{2,1} = 0$. It is important to note that the characteristic functions, F_1 and F_2, do not depend on the boundary conditions at the film periphery.

For the determination of the dispersion relationship two boundary conditions at $r = R$ are needed in order to specify the two constants A_1 and A_1. The non-trivial solution of the problem gives the stability thickness, h_{st}, which is the largest root. Because of the exact form of the characteristic functions, no numerical problems appear. As a first boundary condition we will use the hypothesis for bounded waves, $H_p = 0$ at $r = R$, and as explained above, the second one can be different depending on the physical assumptions. Our calculations showed that the stability thickness does not depend significantly on the second boundary condition applied at the film rim.

To compare both methods for calculation of the stability thickness we calculated h_{st} using the data from Gumerman and Homsy [18] and Scheludko and Manev [36]

for foam film with tangentially immobile interfaces. The parameters of the system are [18,36]: $A_H = 10^{-19}$ J, $P_c = 73$ N/m^2, $\sigma = 65$ mN/m, $R = 100$ μm. The stability thickness calculated by Gumerman and Homsy [18] is 50 nm and our result is 56.7 nm — the small difference between two values is due to the slow convergence of the numerical scheme used by Gumerman and Homsy [18]. The reported measured critical thickness is 27 nm [36]. Therefore, the calculations give approximately two times larger stability thickness than the critical thickness of rupture. One of the reasons for such a big difference is the very high value of the Hamaker constant. To elucidate this point we calculated h_{st} for tangentially immobile interfaces as a function of the film radius, R, by accounting for the electromagnetic retardation [37] in the van der Waals attraction. In Fig. 2 the diamonds represent the values of the stability thickness calculated with $A_H = 10^{-19}$ J and the dots are the results for h_{st} when the Hamaker constant is replaced by its effective value calculated by the relationship [37]:

$$A_{eff}(h) = \frac{3\hbar\omega}{4\pi}\frac{(n_1^2 - n_3^2)^2}{(n_1^2 + n_3^2)^{3/2}}\int_0^\infty \frac{(1 + 2\tilde{h}x)e^{-2\tilde{h}x}}{(1 + 2x^2)^2}dx \tag{24}$$

where $\tilde{h} = 2\pi h\omega n_3(n_1^2 + n_3^2)^{1/2}a$, $\hbar = 6.63 \times 10^{-34}$ J s is the Planck constant, a is the velocity of light in vacuum, $\omega = 3 \times 10^{15}$ Hz is the main electronic absorption frequency, and n_1 and n_3 are the refractive indexes of the disperse and the continuous phases, respectively. The calculated value of A_{eff} is of the order of 10^{-20} J, which is 10 times smaller than the value used in Gumerman and Homsy [18]. At that film thickness the dependence of A_{eff} on h is essential, which results in different slopes of the two curves (Fig. 2). Calculations are performed for interfacial tension $\sigma = 65$ mN/m. The general trend of increase of the stability thickness with the film radius, known from the experiments, is verified.

To illustrate the influence of surfactants we calculated h_{st} as a function of the interfacial tension (Fig. 3). The three curves in Fig. 3 correspond to $\sigma = 30$, 45 and 60 mN/m. It is seen that the decrease of the interfacial tension increases the stability thickness, h_{st}. The presence of surfactants changes also the interfacial mobility. However, all our calculations for real systems did not show any significant dependence of the stability thickness on the mobility of the interfaces (see Section 4).

Since the film continues to drain after the initiation of an unstable state, the present section gives only the upper limit of the critical thickness. The calculation of the critical thickness of bounded films requires very complicated mathematical procedures, which need full non-linear modelling of the evolution of the film profile. This analysis is easier to perform for unbounded waves and the results in Section 4 show that the critical wavelength for unbounded waves is much smaller than the film radius. Therefore, the critical thickness of bounded films will not differ considerably from the critical thickness calculated on the base of unbounded wave analysis.

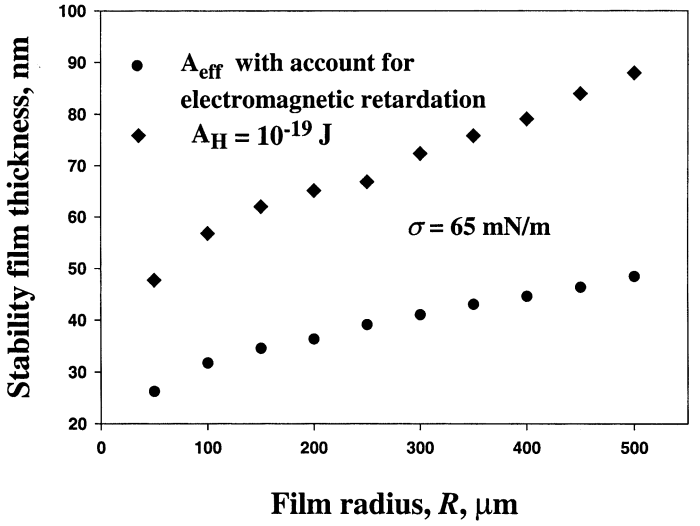

Fig. 2. Influence of the van der Waals attraction and the film radius, R, on the stability thickness for radially-bounded waves.

3.2. Unbounded waves: stability, transitional and critical thickness

In general, the perturbations of the film interfaces can result from uncontrol-

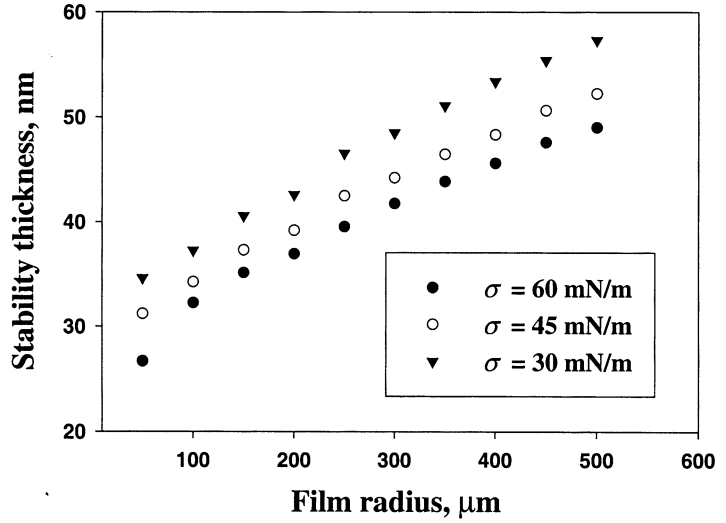

Fig. 3. Influence of the interfacial tension, σ, on the stability thickness for radially-bounded waves.

lable processes such as mechanical disturbances, vibrations, dust, etc., and the film thickness at the rim can also fluctuate. This is one of the physical reasons for investigation unbounded waves.

The main difficulty for solution of the linear problem [Eqs. (16) and (17)] is due to the dependence of the dynamic pressure term on r [the second term in Eq. (17)]. To avoid this problem the perturbations will be presented in the following form:

$$H_p = \int_0^\infty H_0(t,k)J_0(\xi kr)kdk, \quad P_p = \int_0^\infty P_0(t,k)J_0(\xi kr)kdk \tag{25}$$

where k is the wave number, H_0 and P_0 are the amplitudes of the images of the perturbations of the film thickness and the dynamic pressure and $\xi(h)$ is a function, which modifies the radial co-ordinate in the standard Hankel transformation [35]. After long and tedious mathematical transformations it can be proven that if the function $\xi(h)$ is chosen to be

$$\xi = h\sqrt{h+d}, \quad d \equiv \frac{h_s}{1+b} \tag{26}$$

then the Hankel image of Eqs. (16) and (17) transforms into:

$$\frac{1}{H_0}\frac{\partial H_0}{\partial t} = -\frac{V}{h}\frac{3(1+b)h+2h_s}{(1+b)h+h_s} - \frac{h^3k^2\xi^2}{12\eta}\left(1+b+\frac{h_s}{h}\right)\left(\frac{\sigma k^2\xi^2}{2} - \Pi'\right)$$
$$\equiv \frac{3V}{h}Y(h,k) \tag{27}$$

The film instability takes place when the time derivative becomes equal to zero, $\partial H_0/\partial t = 0$. Fig. 4 shows the typical behaviour of Y as a function of the dimensionless wave number $k\xi R/\alpha_1$, for three different values of the thickness of a film with tangentially immobile surfaces. If $Y < 0$ the film is stable while for $Y > 0$ the film is unstable. It is seen that Y has a maximum and the instability first appears at a distance $h = h_{st}$, at which the maximum of the function is equal to zero, i.e. $\max_k(Y) = 0$. By differentiating Y from Eq. (27) with respect to k one finds that the value of the stability wave number, k_{st}, satisfies the condition

$$k_{st}^2\xi_{st}^2 = \Pi'_{st}/\sigma \tag{28}$$

From Eqs. (13) and (27) the corresponding stability thickness becomes a solution of the following transcendental equation:

$$\frac{3h_{st}+2d}{h_{st}+d} = \frac{h_{st}R^2(\Pi'_{st})^2}{16\sigma(P_c - \Pi_{st})} \tag{29}$$

It follows from Eq. (29) that the surfactant influences the stability thickness in three different ways: (i) by reducing the interfacial tension, σ; (ii) by changing the

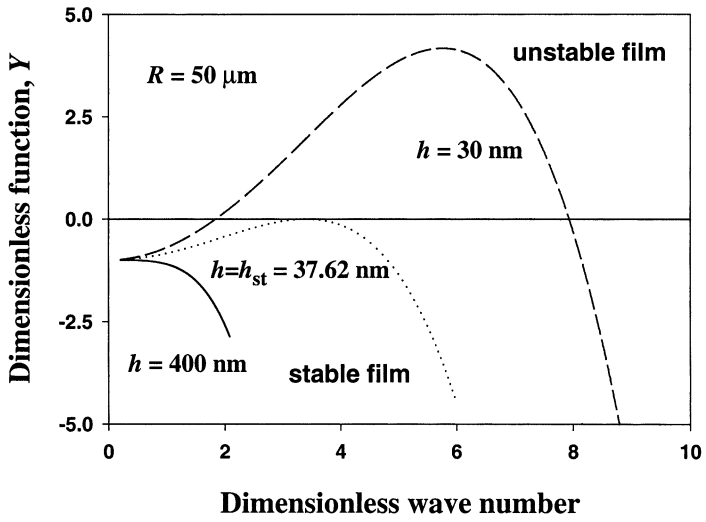

Fig. 4. Typical behaviour of the dimensionless function Y on the dimensionless wave number, $k\xi R/\alpha_1$ for tangentially immobile interface $h = h_{st} = 37.62$ nm corresponds to the stability thickness.

disjoining pressure, Π; and (iii) by suppressing the interfacial mobility. All effects concerning the mobility of the interfaces (surface and bulk diffusion, Gibbs elasticity, etc.) are gathered in one parameter, d, defined through Eq. (26). The right-hand side of Eq. (29) changes from 3 (for tangentially immobile interfaces when $d \ll h_{st}$) to 2 (for very low surfactant concentrations when $d \gg h_{st}$) and therefore, the effect (iii) does not considerably influence the film stability.

Another important conclusion from Eq. (27) is related to the role of the coupling term, the one proportional to the thinning rate V. Since the number of surface waves in an unbounded film is infinite, for a given thickness h (i.e. for a given Π') there will always be waves for which $\sigma k^2\xi^2 \leq 2\Pi'$. According to Frenkel's equation [Eq. (1)] such waves would have been unstable in a non-draining film. For a draining film the respective term [the second one in the middle equation of Eq. (27)] becomes positive but it is not the only one to determine the stability, because it is counterbalanced by the negative coupling term. Hence, instability will occur only when the disjoining pressure effect becomes large enough to overcome the stabilizing effect of the coupling term.

In the particular case of tangentially immobile surfaces and large capillary pressure, $P_c \gg \Pi$, by using the simple form of the van der Waals disjoining pressure, Eq. (3), one can derive an exact solution of the transcendental Eq. (29):

$$h_{st} = \left(\frac{A_H^2 R^2}{192\pi^2\sigma P_c}\right)^{1/7} \approx 0.3402\left(\frac{A_H^2 R^2}{\sigma P_c}\right)^{1/7} \tag{30}$$

The comparison between Eq. (30) and the critical thickness predicted from Eq. (4) (called here $h_{cr,VO}$ [17]) shows that $h_{st} > h_{cr,VO}$.

As discussed in Section 1, the stability thickness indicates only the moment of appearance of the first unstable wave. Its wave number is not arbitrary because it is determined by Eq. (28). If, however, for some reason we select another wave with a given wave number, k, it will become unstable at a thickness smaller than the stability thickness, defined by Eq. (29). However, since the velocity of the fluctuation at the moment, when it becomes unstable, is zero, finite time is needed for the perturbation to develop. During this time the film will continue to thin and finally will break at a smaller critical thickness, $h_{cr} < h_{st}$. To calculate h_{cr} we will combine the simple physical picture, given in Ivanov et al. [12], with the strict mathematical procedure from Williams and Davis [14] and Wit et al. [15].

It is important to realize that the rate of corrugation growth of a given wave, $\partial H_0/\partial t = 0$, depends strongly on the wave number, k, so that waves that became unstable earlier will not necessarily have larger amplitudes, H_0, at the moment of rupture. Hence, one must determine which one is the dominant wave in the moment of rupture — we will call it critical wave. Of course, the shape of the film is determined by the superposition of all possible waves and Vrij has developed a procedure to account for it [11]. It was shown, however [12], that the critical wave plays a dominant role, so that for the sake of simplicity we will confine our treatment below only to this.

Then the procedure from Ivanov et al. [12] is reduced to four main steps.

(1) *Calculate the shapes of all waves at $h = h_{cr}$, i.e. at the moment of film rupture*. This is done by integrating Eq. (27) from the transitional thickness of the respective wave, $h_{tr}(k)$, when it became unstable, until the moment when the average (unperturbed) thickness of the film became equal to the critical thickness of rupture of the film, h_{cr}. When performing the integration, we will use the quasi-steady approximation formulated in [21] according to which the film shape, H_0, depends on time t only implicitly through the average thickness, $h(t)$. Then

$$\frac{\partial H_0}{\partial t} = \frac{\partial H_0}{\partial h}\frac{\mathrm{d}h}{\mathrm{d}t} = -V\frac{\partial H_0}{\partial h} \tag{31}$$

The result of the integration reads

$$\ln H_0(h_{cr},k) - \ln H_0(h_{tr},k) = -\int_{h_{tr}}^{h_{cr}} \frac{3(1+b)h + 2h_s}{(1+b)h + h_s}\frac{dh}{h} + \int_{h_{tr}}^{h_{cr}} \frac{R^2k^2\xi^2}{8(P_c - \Pi)}\left(\Pi' - \frac{\sigma k^2\xi^2}{2}\right)dh \tag{32}$$

where $H_0(h_{cr},k)$ and $H_0(h_{tr},k)$ are the amplitudes of the respective wave at the indicated thicknesses.

(2) *Determine the critical wave, i.e. the wave number k_{cr} of the wave with maximum amplitude H_0 at $h = h_{cr}$*. This is achieved by differentiating Eq. (32) with respect to

k. If one neglects the immaterial dependence of $H_0(h_{tr},k)$ on k (see below) one thus obtains:

$$k_{cr}^2\sigma\int_{h_{tr}}^{h_{cr}}\frac{\xi^4}{P_c-\Pi}dh=\int_{h_{tr}}^{h_{cr}}\frac{\xi^2\Pi'}{P_c-\Pi}dh \tag{33}$$

(3) *Calculate the transitional thickness of the critical wave*. It is the solution of Eq. (27) for $\partial H_0/\partial t=0$ and $k=k_{cr}$:

$$\frac{3h_{tr}+2d}{h_{tr}+d}+\frac{R^2k_{cr}^2\xi_{tr}^2h_{tr}}{8(P_c-\Pi_{tr})}\left(\frac{\sigma k_{cr}^2\xi_{tr}^2}{2}-\Pi'_{tr}\right)=0 \tag{34}$$

(4) *Calculate the amplitude of the critical wave, $H_0(h_{cr},k_{cr})$, in the moment of rupture, which is assumed equal to the critical thickness itself*. This is achieved by setting in Eq. (32) $H_0(h_{cr},k_{cr})=h_{cr}$ and using Eq. (33) for k_{cr}. The result is:

$$\begin{aligned}\ln h_{cr}-\ln H_0(h_{tr})=&-\int_{h_{cr}}^{h_{tr}}\frac{3(1+b)h+2h_s}{(1+b)h+h_s}\frac{dh}{h}\\&+\frac{R^2}{16\sigma}\left[\int_{h_{cr}}^{h_{tr}}\frac{\xi^2\Pi'dh}{(P_c-\Pi)}\right]^2\left(\int_{h_{cr}}^{h_{tr}}\frac{\xi^4dh}{P_c-\Pi}\right)^{-1}\end{aligned} \tag{35}$$

where $h_{tr}(k_{cr})$ is provided by Eq. (34). In the general case this equation for h_{cr} can be solved only numerically. The hypothesis $H_0(h_{cr},k_{cr})=h_{cr}$ leads to extension of the linear stability theory into the non-linear regime, which is not proper mathematically. Nevertheless, for van der Waals disjoining pressure this provides correct results (see Section 4).

The only unknown parameter in Eq. (35) is the initial amplitude of the fluctuations, $H_0(h_{tr})$. In Ivanov et al. [12] and Vrij and Overbeek [17] the initial amplitudes are determined from the Einstein theorem, which is applicable only to thermal fluctuations. This means that it is assumed that in the moment, when a given wave becomes unstable, i.e. at its transitional thickness, it has the same amplitude as it would have had at a single interface. This gives $H_0(h_{tr})\approx\sqrt{k_BT/\sigma}\approx 0.1\div 0.5$ nm. In Williams and Davis [14] and Wit [15] the amplitudes are chosen to be approximately 0.1 nm because the perturbations in general are result from uncontrollable processes (mechanical disturbances). Our computations show that if $H_0(h_{tr})$ varies from 0.1 to 0.5 nm the critical thickness does not change considerably.

In the case of tangentially immobile interfaces and the simple form of the van der Waals interaction, Eq. (3), the integrals in Eqs. (33) and (35) can be evaluated exactly. Unfortunately these results are not applicable for quantitative calculation of the critical thickness because for film thickness from 20 to 40 nm A_{eff} strongly depends on h [see Eq. (24) and the discussions in Section 3.1].

4. Numerical results and discussion

In this section the results from the linear stability analysis for the two wave modes (bounded and unbounded waves) are compared. The influence of the different factors on h_{st}, h_{tr} and h_{cr} is investigated and the numerical results are checked against experimental data for stability of foam and emulsion films.

Surfactants damp the interfacial mobility thus decreasing the velocity of film thinning, V. That is why when the surfactant concentration decreases, the rate of thinning increases [see Eq. (13)]. The surfactant has the same effect on the corrugation growth rate $\partial H_0/\partial t$ for non-draining films. Indeed, if in the first term of the middle equation in Eq. (27) one sets $V = 0$ (non-draining film) one sees that the only remaining term in the expression for the growth rate is multiplied by the same mobility (surfactant dependent) factor $1 + b + h_s/h$. This increase of the growth rate with the decreasing surfactant concentration for non-draining films may lead to the wrong conclusion that in draining (thinning) films, also the amplitude of the wave will increase much faster with decreasing surfactant concentration and thereby — the critical thickness will considerably increase. This is so, but the effect is much smaller than could be expected. With draining films the surfactant affects only the coupling term in the expression [Eq. (35)] for the critical thickness. This term is not very significant even for films with tangentially immobile surfaces (see Fig. 9 and the corresponding discussion below), so that the effect of the surface mobility on the stability, transitional and critical thicknesses is negligible. This is demonstrated in Fig. 5 showing the relative change of the stability, transitional and critical thicknesses, h/h_{im}, with respect to their values for tangentially immobile interfaces, h_{im}, as a function of the mobility parameter, d (see Section 3.1). The foam film radii are 100 μm and 500 μm, the radius of the capillary is $R_c = 1.79$ mm, the interfacial tension is constant, 30 mN/m, and the calculations are performed by using the effective constant A_{eff} for the van der Waals attraction, Eq. (24). In spite of the wide range of the interfacial mobility parameter, the relative change of all calculated thicknesses is not higher than 0.055. Two general tendencies are demonstrated — the increasing of the interfacial mobility leads to slight increase of the critical thickness and for the large films the relative change becomes less pronounced (see Fig. 5).

These results have simple physical interpretations. It is obvious from Eq. (31) that the critical thickness is determined by the ratio of the velocity of wave growth and film thinning. By increasing the surface mobility we increase the corrugation growth rate but since at that the film thins faster, the waves have less time to reach the moment when the two interfaces touch each other. As a result the wave amplitudes in this moment are not much different from what they would have been with smaller growth rates but also, with slower thinning. Hence, the critical thickness is almost the same. It should be emphasized that this is so only because, as explained above, the surfactant affects the thinning rate V and the wave growth (without the coupling term) in exactly the same way. The situation could be substantially different if the surfactant exhibits noticeable surface viscosity, η_s. The effect of the latter is inversely proportional to the square of the radial scale length

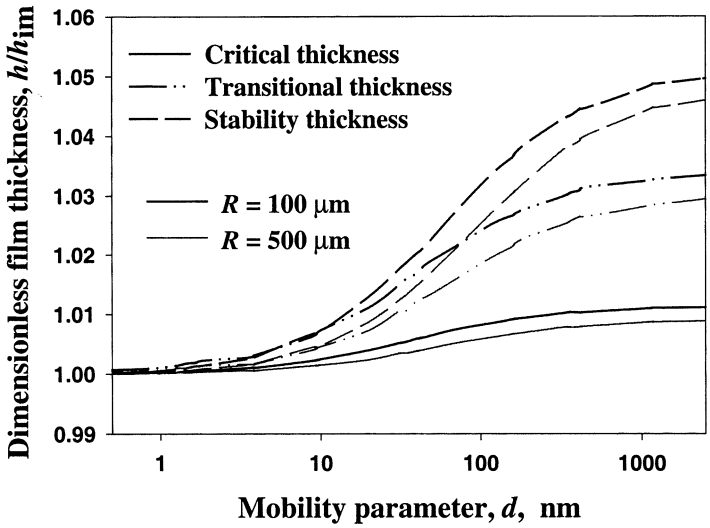

Fig. 5. Role of the interfacial mobility on the stability, transitional and critical thicknesses for different film radii.

(see [42]), which is the film radius R for the thinning rate and the wavelength λ for the corrugation growth. Since typically $\lambda = 0.1\ R$ (see Fig. 8) it is possible that with some intermediate values of the surface viscosity, η_s, it simultaneously has no effect on the drainage rate but damps strongly the wave growth. This problem is discussed in more detail elsewhere [42].

The relative changes of the critical and stability wave numbers, k/k_{im}, are plotted in Fig. 6. It is seen that the film radius does not significantly influence the wave numbers. While the relative stability wave numbers drop slightly, the relative critical wave numbers change approximately 10 times with increasing interfacial mobility. Therefore, the longer waves become more dangerous for low surfactant concentrations.

Another physico-chemical parameter, which affects the stability of the drainage film, is the interfacial tension. From Eq. (13) it follows that for higher values of σ the thinning velocity increases due to the larger capillary pressure, P_c. Therefore, the interfacial tension influences the film stability in two ways: by the capillary damping of fluctuations and by increasing the stabilization role of the drainage flow. In Fig. 7 are presented the numerical results for h_{st}, h_{tr} and h_{cr} as a function of the film radius, R, and the interfacial tension, σ. The calculations are carried out for foam films and tangentially immobile interfaces. The other parameters are the same as in Figs. 5 and 6. As one can expect, the film is more stable for higher interfacial tension and all calculated thicknesses ($h_{st} > h_{tr} > h_{cr}$) increase with the film radius. For small film radii the differences between the three thicknesses falls down and especially for slightly deformed drops they can be negligible [25]. The

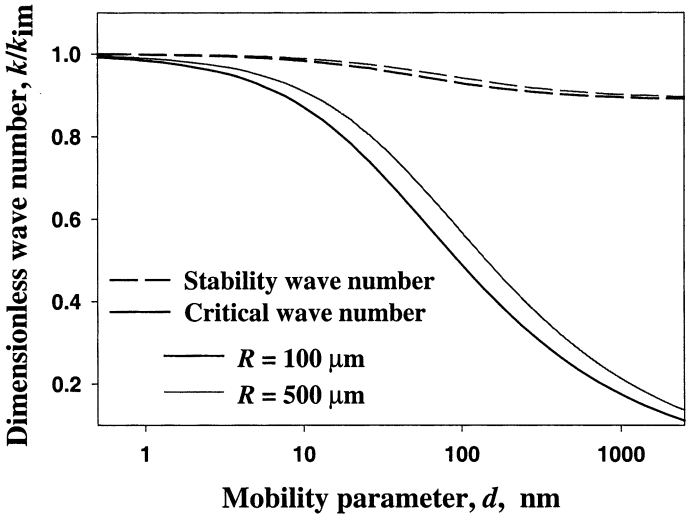

Fig. 6. Dimensionless stability and critical wave numbers as a function of the interfacial mobility for different film radii.

characteristic values of the stability and the critical wavelengths, $\alpha_1/(k\xi)$, calculated for the system from Fig. 7, as a function of R are shown in Fig. 8. The curves illustrate the relationship between the wavelength of the perturbations and the film radius. It is interesting to note that there is no considerable difference between the wavelengths calculated at different values of the interfacial tension. The wavelengths increase with the film radii and the critical wavelength is always smaller than that at the boundary of film stability. Figs. 7 and 8 show that for all film radii the wavelengths are much larger than the film thicknesses, i.e. the long wave approximation is applicable. The critical wavelength is approximately 10 times smaller than the film radii, which means that the amplitude of the fluctuations decreases significantly at the film rim. Vrij's formula [17] for the critical wavelength is $\lambda_c \approx 0.21\ R$. It shows linear dependence from the film radius. The characteristic critical wavelength in our case (Fig. 8) has more complicated dependence on the film radius and the characteristic wavelength is smaller than those predicted in Vrij and Overbeek [17]. For smaller film radii the wavelength decreases slower than the decrease of R and at $R = 5$ μm it becomes equal to R. Therefore, films with radii smaller than 5 μm are stable with respect to fluctuations.

The most precise criterion for the applicability of the approaches for bounded and unbounded waves, described in Section 3, is a comparison with experimental data. All calculated thicknesses (stability, transitional and critical thickness from Section 3.2, stability thickness from Section 3.1 and those calculated using the Vrij and Overbeek [11,17] approach) are plotted in Fig. 9. The experimentally obtained values [32] for the critical thickness for aqueous foam films containing 4.3×10^{-4} M sodium dodecyl sulfate (SDS) and 0.25 M NaCl as a function of the film radius

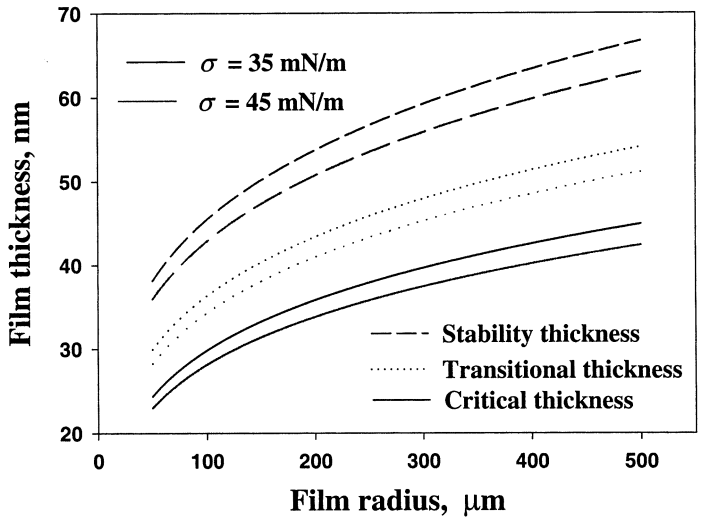

Fig. 7. Dependence of the stability, transitional and critical thicknesses on the interfacial tension and film radii.

are also presented in Fig. 9. The experimental parameters, describing the system, as well as the measured and calculated critical thicknesses are given in Table 1. All numerical results are obtained by using A_{eff} from Eq. (24) with the respective refractive indexes of air and water. Therefore, all parameters, which are needed for

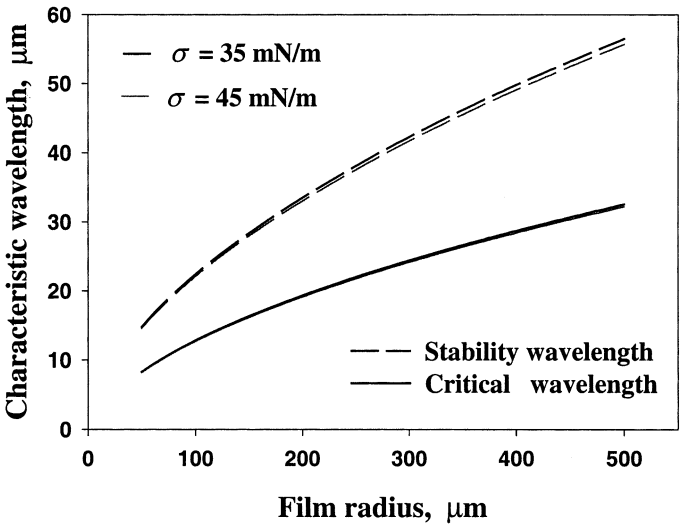

Fig. 8. Stability and critical characteristic wavelengths vs. film radius for different interfacial tensions.

Table 1
Comparison of experimental and theoretical values of critical thickness of film rupture for aqueous foam films stabilized by 4.3×10^{-4} M SDS + 0.25 M NaCl: $\sigma = 37$ mN/m, $R_c = 1.79$ mm and $P_c = 41.3$ mN/m^2 [32]

Film radius R (μm)	Critical film thickness (nm)		
	Experiment	Linear analysis	Non-linear analysis
50	25	24.15	25.20
100	30	29.57	30.72
200	35	35.54	36.71
300	40	39.34	40.55
500	47	44.53	45.80

For the results from non-linear analysis see Section 4.

the calculation are known — we have no adjustable parameter. In order to have an adequate comparison between all discussed models [11,12,17–19], everywhere A_H is replaced by A_{eff} and therefore, the stability thicknesses calculated here (from the model in Section 3.1) differ from those of Malhotra and Wasan (see Fig. 6 in Malhotra and Wasan [19]). Moreover, in Malhotra and Wasan [19] A_H is an adjustable parameter. The following conclusions can be drawn from Fig. 9 and Table 1. As can be expected from Section 3.2 the following relationship between the thicknesses holds: $h_{st} > h_{tr} > h_{cr}$. The calculated critical thicknesses pass through all experimental data and an excellent agreement is found. The stability thickness from the model of the bounded waves is very close to the transitional

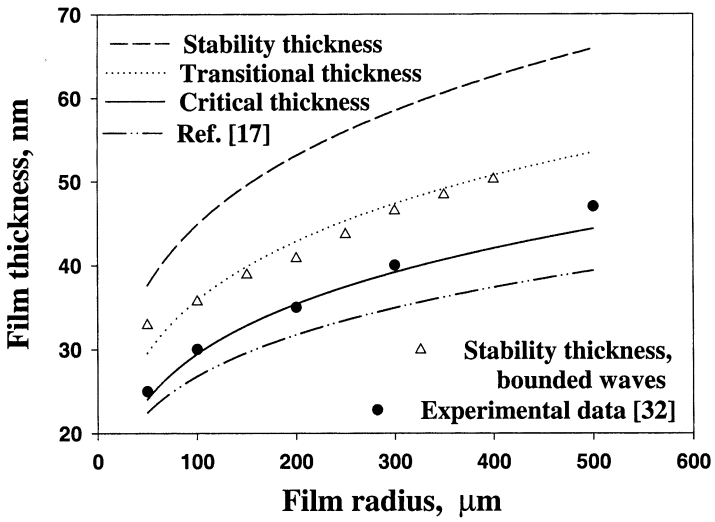

Fig. 9. Stability, transitional and critical thicknesses of foam film calculated from the different models and comparison with the experimental data [32]. The parameters of the system are given in Table 1.

Table 2
Comparison of experimental and theoretical values of critical thickness of film rupture for aqueous emulsion films stabilized by 4.3×10^{-4} M SDS + 0.1 M NaCl: $\sigma = 7.9$ mN/m, $R_c = 1.58$ mm and $P_c = 10$ mN/m^2 [32]

Film radius R (μm)	Critical film thickness (nm)		
	Experiment	Linear analysis	Non-linear analysis
50	25	23.02	24.08
70	27	25.41	26.46
100	30	28.06	29.11
150	32	31.23	32.31
200	35	33.61	34.71
300	38	37.15	38.30

For the results from non-linear analysis see Section 4.

thicknesses and, as it should be, the values are larger than the experimental ones. The corresponding values of the critical thicknesses from the model of Vrij and Overbeek [11,17] are lower than the experimental data for all film radii. This result comes from the neglect of the coupling between the drainage and fluctuation flows in Vrij [11] and Vrij and Overbeek [17].

Another experimental system, reported in Manev et al. [32], is aqueous emulsion films containing 4.3×10^{-4} M SDS + 0.1 M NaCl with toluene as dispersed phase (see Table 2 for experimental parameters and data). The calculated stability,

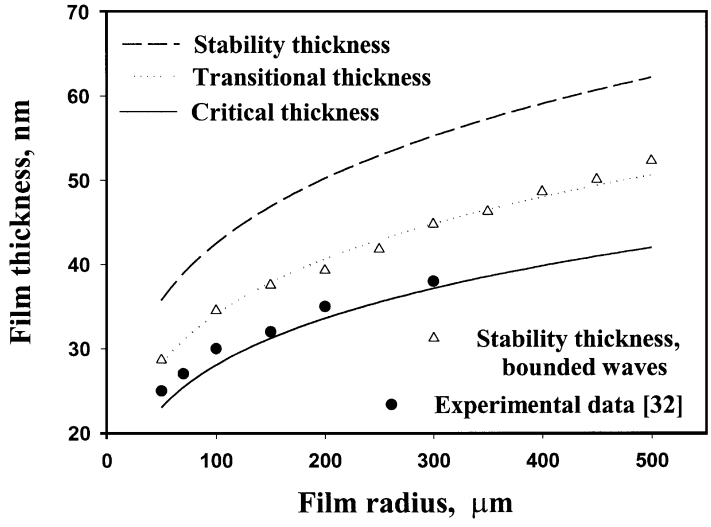

Fig. 10. Comparison between the stability, transitional, critical and stability (bounded waves) thicknesses and the experimental data [32] for emulsion film. The parameters of the system are given in Table 2.

transitional and critical thicknesses and the experimental data are plotted in Fig. 10. Again we have no adjustable parameter (for the calculation of A_{eff} the refractive index of toluene was 1.4969). In spite of the much smaller interfacial tension and van der Waals attraction in comparison with the ones for foam systems (Fig. 9), the calculated critical thickness describes, again very well, all experimental data. The obtained stability thicknesses of bounded waves and the transitional thicknesses almost coincide (Fig. 10) as it was for foam films. This fact could not be proven mathematically — it is the result only of numerical calculations.

The criterion for film rupture, $H_0(h_{\text{cr}}) = h_{\text{cr}}$, used in Section 3.2, does not obey the main assumption in the linear stability analysis, namely that the perturbations are small. This raises doubts whether the results obtained by linear stability analysis are adequate. The issue is illustrated in Fig. 11, showing the disjoining pressure isotherm $\Pi(h)$ for a film exhibiting attractive van der Waals disjoining pressure at large thicknesses h, but strong short range (steric) repulsion at very small thicknesses. Imagine now a film thinning under the action of the capillary pressure P_c and the disjoining pressure Π, i.e. under the action of driving pressure $P_c - \Pi$. At the point NBF, $P_c = \Pi$ and a very thin equilibrium film, called Newton Black Film (NBF) must form. However, the observations of de Vries showed [10] that it does not form through gradual thinning of the thicker film, but as depicted in the inset A in Fig. 11, through the formation of small, very thin 'black spots', which are nuclei of the NBF. De Vries surmised that their mechanism of formation is the same as that of film rupture, i.e. they are formed through local corrugation and instability of the thicker film (inset B in Fig. 11), but when the two surfaces 'touch' each other the repulsive disjoining pressure is strong enough to counterbalance the attractive van der Waals disjoining pressure. If the repulsive interaction is still present, but not large enough to prevent rupture, it can still slow it down, in the mean time the film may additionally thin and the critical thickness of

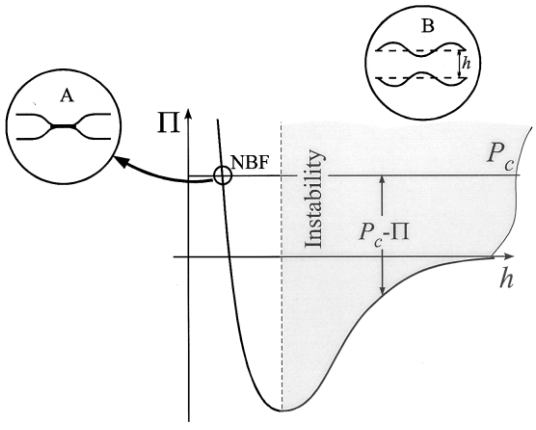

Fig. 11. Disjoining pressure of a film with short-range repulsion. Scheme of the formation of 'black spots' and their role on the critical thickness of rupture.

rupture will be lower than the one calculated from the linear analysis by accounting only for the attractive interactions. This picture will be approximately the same for any repulsive interaction, if it has shorter range than the attractive interaction. For example, in the case of ionic surfactants, when the concentration of the background electrolyte is not high enough to shrink the electrical double layer, the electrostatic interactions become operative at film thicknesses smaller than 30–40 nm. However, from Figs. 9 and 10 we see that $h_{cr} \geq 25$ nm, i.e. it is comparable with the thickness range where the repulsive electrostatic disjoining pressure is operative, so that again it will affect the value of the critical thickness of rupture.

Unfortunately, it is not possible to account for the repulsive part of $\Pi(h)$ in the linear stability analysis, because the boundary conditions are formulated at the unperturbed film surfaces at $z = \pm h/2$ (see Fig. 1 and inset b in Fig. 11) in the instability region (where $d\Pi/dh > 0$, the shaded area in Fig. 11). Hence, the value of Π', used in the theory, corresponds to this region and do not account for the strong repulsive $\Pi(h)$ at smaller thicknesses. The only way to answer the question to what extent the results from the linear theory are correct is to apply the non-linear stability analysis (for more details on this method see the literature [14,15,38–41]). Since the numerical procedures involved at that are very much time consuming, they can be applied only for investigation of specific cases, not for full scale investigation of the influence of all possible physicochemical parameters. The main steps of the algorithm of the non-linear theory are the following. The series in Eq. (10) and the basic state solution [Eqs. (11)–(13)] are substituted into the integrated mass balance [Eq. (5)] and the tangential and normal stress boundary conditions Eqs. (6) and (9). The resulting non-linear system represents the evolution problem for the fluctuations. The initial conditions are chosen from the linear theory, i.e. the fluctuation mode in the film profile is proportional to the zeroth-order Bessel function, $J_0(kr)$. The numerical method for solution of the strongly non-linear partial differential equations of the evolution problem is described in Paunov et al. [41]. Essentially, it consists of selecting a set of different modes with different initial film thicknesses, h_{init} and different rupture times, τ_r. The most unstable mode defines the critical time of film rupture, $\tau_r \equiv \min_{h_{init},k}[\tau_r(h_{init},k)]$, the critical wave number, k_{cr}, and the thickness at which the critical mode becomes initially unstable, i.e. h_{tr}. The film thickness, which corresponds to τ_{cr}, is the critical thickness of the film as a whole, h_{cr}.

The numerical results from the non-linear stability analysis for the foam and emulsion systems from Figs. 9 and 10 are given in Tables 1 and 2. It is seen that for these systems the critical thicknesses, predicted from the non-linear stability analysis, are only slightly higher than those from Section 3.2. The calculated values of h_{cr} from the linear and non-linear stability analyses virtually coincide with all experimental points and therefore, both theories are applicable for prediction of the film stability when the van der Waals interaction is the main part of the disjoining pressure.

In Jain and Ivanov [43] one possible reason was suggested why the linear stability analysis gives correct results for h_{cr} even though it is applied when it is definitely not valid, in the moment of rupture, when $H_0 \cong h$. It is apparent from Eqs. (31)

and (32) in Section 3.2, that the critical thickness value is determined by $(\partial H_0/\partial t)/V$, i.e. by the ratio of the rate of wave growth and the rate of thinning. For van der Waals interactions this ratio strongly increases with the decrease of the film thickness, h, once the critical wave has become unstable and is much larger than unity at $h \geq h_{cr}$, i.e. the wave corrugation crosses so quickly the 'dangerous zone', where the linear analysis is not valid, that the film has virtually no time to thin in this zone and the value of the critical thickness is only slightly affected by the violation of the approximation.

5. Conclusions

Several approaches to describe the stability of thin draining films are analysed: linear and non-linear stability analyses and bounded and unbounded wave modes. The evolution of a draining film passes through the following stages. At a thickness h_{st} the film loses its marginal stability and the first unstable wave mode appears — after this moment the film continues to drain and the spectrum of the unstable modes becomes wider. At a given moment, corresponding to the transitional thickness, h_{tr}, the critical wave, which has the maximum amplitude at the moment of rupture, becomes unstable. Afterwards the film keeps thinning and the amplitude of the critical wave grows up to the moment when the film surfaces 'touch' each other and the film ruptures — this occurs at the critical thickness, h_{cr}. The non-linear stability analysis gives similar results for the critical thickness as the linear one when only the van der Waals disjoining pressure is operative.

The surfactants modify the mobility of the interfaces and damp the velocity of film drainage. However, the interfacial mobility does not affect considerably the critical film thickness — the interfacial tension, the film radius and the disjoining pressure are the main physicochemical properties, which affect the film stability. The larger the van der Waals interaction and the film radius, the more unstable the draining film is. The excellent agreement between the experimental data and the calculated values of h_{cr} from linear stability analysis (Sections 3.2 and 4), achieved without using any adjustable parameter, demonstrates the applicability of the proposed theory. The electromagnetic retardation effect in the van der Waals interaction has to be taken into account when experimental data are processed. The neglect of the coupling between the drainage and fluctuation flows [11,12,17] overstates the film stability — the calculated critical thicknesses are somewhat smaller than the experimental data. The stability analysis of bounded wave, performed in [18,19] actually gives only the moment of onset of the instability. The thickness, at which this occurs, is always larger than the real critical thickness.

Acknowledgements

This study was funded by the Inco-Copernicus Project IC15CT980911. The authors are grateful for this financial support.

References

[1] I.B. Ivanov, P.A. Kralchevsky, Colloids Surf. A: Physicochem. Eng. Aspects 128 (1997) 155.
[2] I.B. Ivanov, K.D. Danov, P.A. Kralchevsky, Colloids Surfaces A: Physicochem. Eng. Aspects 152 (1999) 161.
[3] Ch. Maldarelli, R. Jain, in: I.B. Ivanov (Ed.), Thin Liquid Films: Fundamentals and Applications, Marcel Dekker, New York, 1988, pp. 497–568.
[4] P.A. Kralchevsky, K.D. Danov, I.B. Ivanov, in: R.K. Prud'homme (Ed.), Foams: Theory, Measurements and Applications, Marcel Dekker, New York, 1996, pp. 1–99.
[5] K.D. Danov, P.A. Kralchevsky, I.B. Ivanov, in: G. Broze (Ed.), Handbook of Detergents. Part A: Properties, Marcel Dekker, New York, 1999, pp. 303–418.
[6] B.V. Derjaguin, V.N. Churaev, V.M. Muller, Surface Forces, Plenum Press, New York, 1987.
[7] V.N. Churaev, Kolloidn. Z. 61 (1999) 462.
[8] V.N. Churaev, Kolloidn. Z. 62 (2000) 581.
[9] J. Frenkel, Kinetic Theory of Liquids, Dover, New York, 1955.
[10] A. de Vries, Rec. Trav. Chim. 77 (1958) 441.
[11] A. Vrij, Discuss. Faraday Soc. 42 (1966) 23.
[12] I.B. Ivanov, B. Radoev, E. Manev, A. Scheludko, Trans. Faraday Soc. 66 (1970) 1262.
[13] C.-Y.D. Lu, M.E. Cates, Langmuir 11 (1995) 4225.
[14] M.B. Williams, S.H. Davis, J. Colloid Interface Sci. 90 (1982) 220.
[15] A.D. Wit, D. Gallez, C.I. Christov, Phys. Fluids 6 (1994) 3256.
[16] A.D. Scheludko, Adv. Colloid Interface Sci. 1 (1967) 391.
[17] A. Vrij, J.Th.G. Overbeek, J. Am. Chem. Soc. 90 (1968) 3074.
[18] R.J. Gumerman, G.M. Homsy, Chem. Eng. Commun. 2 (1975) 27.
[19] A.K. Malhotra, D.T. Wasan, Chem. Eng. Commun. 48 (1986) 35.
[20] I.B. Ivanov, D.S. Dimitrov, in: I.B. Ivanov (Ed.), Thin Liquid Films: Fundamentals and Applications, Marcel Dekker, New York, 1988, pp. 379–496.
[21] I.B. Ivanov, D.S. Dimitrov, P. Somasundaran, R.K. Jain, Chem. Eng. Sci. 40 (1985) 137.
[22] G. Singh, G.J. Hirasaki, C.A. Miller, J. Colloid Interface Sci. 184 (1996) 92.
[23] K.D. Danov, D.S. Valkovska, I.B. Ivanov, J. Colloid Interface Sci. 211 (1999) 291.
[24] D.S. Valkovska, K.D. Danov, I.B. Ivanov, Colloids Surf. A: Physicochem. Eng. Aspects 156 (1999) 547.
[25] D.S. Valkovska, K.D. Danov, I.B. Ivanov, Colloids Surf. A: Physicochem. Eng. Aspects 175 (2000) 179.
[26] D.S. Valkovska, K.D. Danov, J. Colloid Interface Sci. 223 (2000) 314.
[27] I.B. Ivanov, Pure Appl. Chem. 52 (1980) 1241.
[28] T.T. Traykov, I.B. Ivanov, Int. J. Multiphase Flow 3 (1977) 471.
[29] T.T. Traykov, I.B. Ivanov, Int. J. Multiphase Flow 3 (1977) 485.
[30] D.S. Valkovska, P.A. Kralchevsky, K.D. Danov, G. Broze, A. Mehreteab, Langmuir 16 (2000) 8892.
[31] G. Guerin, Second World Congress on Emulsion, Bordeaux, Congress Proceedings, 4 (1977) 337–344.
[32] E.D. Manev, S.V. Sazdanova, D.T. Wasan, J. Colloid Interface Sci. 97 (1984) 591.
[33] D. Exerowa, P. Kruglyakov, Foam and Foam Films. Theory, Experiments, Application, Elsevier, Amsterdam, 1998.
[34] S.A.K. Jeelany, S. Hartland, J. Colloid Interface Sci. 164 (1994) 296.
[35] G. Arfken, Mathematical Methods for Physicists, Academic Press, Boston, MA, 1985.
[36] A. Scheludko, E. Manev, Trans. Faraday Soc. 64 (1968) 1123.
[37] W.B. Russel, D.A. Saville, W.R. Schowalter, Colloidal Dispersions, Cambridge University Press, Cambridge, 1989.
[38] K.D. Danov, N. Alleborn, H. Raszillier, F. Durst, Phys. Fluids 10 (1998) 131.
[39] K.D. Danov, V.N. Paunov, N. Alleborn, H. Raszillier, F. Durst, Chem. Eng. Sci. 53 (1998) 2809.

[40] K.D. Danov, V.N. Paunov, S.D. Stoyanov, N. Alleborn, H. Raszillier, F. Durst, Chem. Eng. Sci. 53 (1998) 2823.
[41] V.N. Paunov, K.D. Danov, N. Alleborn, H. Raszillier, F. Durst, Chem. Eng. Sci. 53 (1998) 2839.
[42] I.B. Ivanov, D.S. Dimitrov, Coll. Polym. Sci. 252 (1974) 982.
[43] R.K. Jain, I.B. Ivanov, JCS Faraday II 76 (1980) 250.